

See discussions, stats, and author profiles for this publication at: <https://www.researchgate.net/publication/234869697>

A Whipping Fluid Jet Generates Submicron Polymer Fibers

Article in *Applied Physics Letters* · February 2001

DOI: 10.1063/1.1345798

CITATIONS

519

READS

130

4 authors, including:



Moses Hohman

University of Chicago

22 PUBLICATIONS 2,949 CITATIONS

SEE PROFILE

Electrospinning: A whipping fluid jet generates submicron polymer fibers

Y. M. Shin

Department of Materials Science and Engineering, Massachusetts Institute of Technology, Cambridge, Massachusetts 02139

M. M. Hohman

James Franck Institute and Department of Physics, University of Chicago, Chicago, Illinois 60637

M. P. Brenner

Department of Mathematics, Massachusetts Institute of Technology, Cambridge, Massachusetts 02139

G. C. Rutledge^{a)}

Department of Chemical Engineering, Massachusetts Institute of Technology, Cambridge, Massachusetts 02139

(Received 26 October 2000; accepted for publication 30 November 2000)

Polymeric fibers with diameters in the range from 50 nm to 5 μm are produced by accelerating a fluid jet in an electric field, in a process known as “electrospinning.” Here we show that an essential element of the process is a fluid instability, the rapidly whipping jet. The phenomena responsible for the onset of whipping are revealed by a linear instability analysis that describes the jet behavior in terms of known fluid properties and operating conditions. The behavior of two competing instabilities, the Rayleigh mode and the axisymmetric conducting mode, is also described. The results are summarized using operating diagrams, delineating regimes of operation in electrospinning, which are in good agreement with experimental observations. © 2001 American Institute of Physics. [DOI: 10.1063/1.1345798]

Electrostatic fiber spinning, or “electrospinning,” is a technology that uses electric fields to produce nonwoven materials that are unparalleled in their porosity, high surface area, and the fineness and uniformity of their fibers. The diameters of electrospun fibers are typically hundreds of nanometers, one to two orders of magnitude smaller than fibers produced by conventional extrusion techniques. These fibers are attracting considerable interest in a wide range of applications, including filters, membranes, composites and biomimetic materials.^{1–4} Despite this surge in interest, the essential features of the process responsible for the formation of such fine fibers have proved elusive to both scientific understanding and engineering control.^{5–7}

Figure 1 shows a scanning electron micrograph (SEM) of submicron diameter fibers of poly(ethylene oxide) (PEO), produced from an aqueous solution by electrospinning. Such fibers are collected as a nonwoven fabric when a charged fluid jet is accelerated down an electric field gradient, solidified, and deposited onto a grounded collector. Similar fibers have been manufactured from over 30 different kinds of polymers in recent years. By contrast, synthetic polymer fibers produced by conventional extrusion-and-drawing processes are typically 10–500 μm in diameter, and are collected on spools for forming yarns or woven textiles.⁸ Controlling the fiber properties requires understanding how the electrospinning process transforms a millimeter-diameter fluid stream into solid fibers four orders of magnitude smaller in diameter. In the conventional view, electrostatic charging of the fluid at the tip of a nozzle results in the formation of the well-known Taylor cone,⁹ from the apex of which a single fluid jet is ejected. As the jet accelerates and

thins in the electric field, radial charge repulsion results in splitting of the primary jet into multiple filaments, in a process known as “splaying.”⁷ In this view, the final fiber size is determined primarily by the number of subsidiary jets formed.

Our studies suggest that the most important element operative during electrospinning is the rapid growth of a non-axisymmetric, or “whipping,” instability that causes bending and stretching of the jet. At low fields, a single, uniformly thinning jet extends from the nozzle to the collector [Fig. 2(a)]. At high fields, after traveling a short distance the jet becomes unstable. Viewed with exposure times down to 1 ms, the unstable region of the jet [Fig. 2(b)] has the appearance of an “inverted cone,” suggestive of the envelope created by multiple jets. Using high-speed photography, we have confirmed that the inverted cone imaged in Fig. 2(b) is in reality a single, rapidly whipping jet^{5,10,11} [Fig. 2(c)]. The whipping frequency is so fast that the jet appears to be

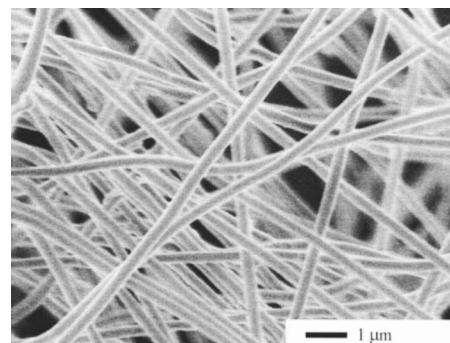


FIG. 1. SEM micrograph of electrospun PEO fibers. The fibers were spun from a 2 wt % solution of PEO (MW=2 000 000) in water at a flow rate of 1 ml/min and an electric field of 0.46 kV/cm. The fibers are deposited in the form of a nonwoven fabric.

^{a)}Electronic mail: rutledge@mit.edu

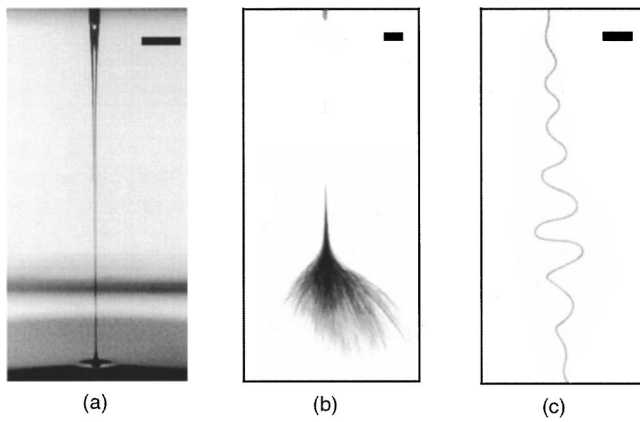


FIG. 2. Jet images of a 2 wt % solution of PEO (MW=2 000 000) in water during electrospinning. (a) Stable jet ($E_\infty=0.5$ kV/cm, $Q=4$ ml/min, scalebar=5 mm); (b) unstable jet ($E_\infty=0.67$ kV/cm, $Q=0.1$ ml/min, scalebar=5 mm, 1 ms exposure); (c) close-up of the onset of instability ($E_\infty=0.67$ kV/cm, $Q=0.1$ ml/min, scalebar=1 mm, 18 ns exposure).

splitting into multiple filaments, a phenomenon observed earlier for electrostatic sprays.¹² In our laboratory, the production of submicron diameter fibers is always preceded by the onset of this whipping instability. The whipping instability is one of several possible instabilities that may occur in an electrified fluid jet. Additional types of instabilities may lead, for example, to breakup of the jet into droplets. Interactions between the free charge in the jet and the external electric field give rise to competition between the different instabilities, which are convected downstream and grow at different rates, depending upon the fluid parameters and the operating conditions. Controlling electrospinning therefore requires a model by which the competition between the fluid instabilities in an electrified fluid jet can be quantified. From this, operating conditions can be found which take advantage of the desired instability.

Our model of the electrospinning process is based on the observation that the instabilities occur with wavelengths much longer than the jet radius, so that the jet can be modeled as a long, slender object. The usual equations for modeling a Newtonian fluid jet—conservation of mass and charge, and differential momentum balance—and the electric field equation are substantially simplified by making an asymptotic expansion in the aspect ratio of the jet and neglecting the higher order terms. Introducing perturbations to the radius, velocity, surface charge distribution, and the local field strength (e.g., of the form $h^*/h = 1 + h_e e^{i\omega t + ikz}$ for the jet radius) leads to a set of equations for the growth rates $\omega(E, h, \sigma)$ of long wavelength distortions of the radius and the centerline of the jet. Here, E is the local electric field, h is the radius of the jet, and σ is the surface charge distribution, all of which vary along the length z of the jet.

In the stability analysis, the surface charge distribution at a distance z from the nozzle is expressed in a multipole expansion. We have solved the growth rate equations arising from monopoles $\sigma(z)$ and from dipoles $P(z)$, which accompany varicose and bending deformations of the jet, respectively. The calculations indicate the possibility for three types of instabilities. The first of these, the classical Rayleigh instability, is axisymmetric; it is suppressed when the applied electric field E_∞ and the surface charge density σ exceed a

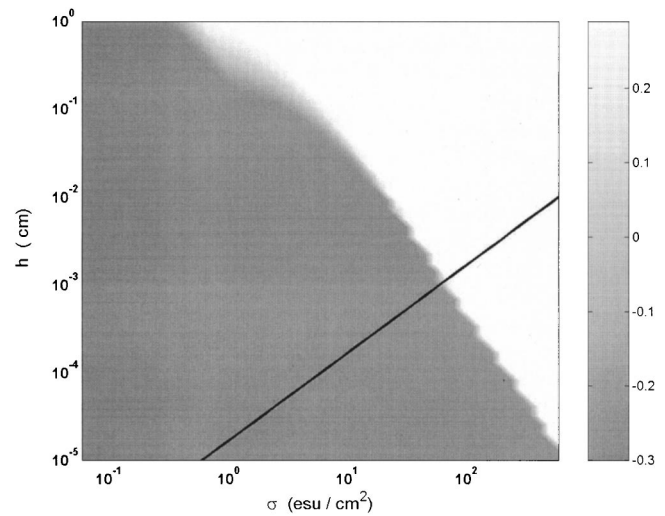


FIG. 3. Theoretical diagram plotting the ratio of whipping mode growth rate to axisymmetric growth rate, $\log_{10}(\omega_w/\omega_a)$, vs σ and h . Light region: $\log_{10}(\omega_w/\omega_a) > 2$; dark region: $\log_{10}(\omega_w/\omega_a) < -2$. The solid line indicates the asymptotic jet path, $\sigma = Ih/2Q$. 2 wt % solution of PEO (MW = 2 000 000) in water. $E_\infty = 2$ kV/cm, $K = 120$ μ S/cm, $\eta = 16.7$ P, $Q = 15$ ml/min, $I = 10$ μ A.

threshold given by $(\epsilon - \bar{\epsilon})E_\infty^2 + 4\pi\sigma^2/\bar{\epsilon} = 2\pi\gamma/h$, where γ is the surface tension, $\epsilon(\bar{\epsilon})$ is the dielectric constant inside (outside) the jet, and $\epsilon/\bar{\epsilon} \gg 1$.¹³ At high field, a second axisymmetric instability and a third, nonaxisymmetric instability, which is due to fluctuations in the dipolar component of the charge distribution, dominate. These “conducting” modes are electrically driven and essentially independent of surface tension. The axisymmetric conducting mode arises as a consequence of the finite, nonzero conductivity of the fluid, which produces an extra root to the growth rate equations. The whipping instability can occur through either: (i) small lateral fluctuations in the centerline of the jet result in the induction of a dipolar charge distribution, as the free charge adjusts to screen out the field inside the jet. The dipoles interact with the external electric field, producing a torque that further bends the jet; and (ii) mutual repulsion of surface charges carried by the jet causes the centerline to bend.

In contrast to previous models,^{11,14} the approach presented here successfully describes the stability characteristics of the jet as a function of realistic and measurable values of the fluid properties and operating parameters. The most important characteristics of the fluid are found to be viscosity and conductivity. The main operating parameters are the applied electric field and flow rate. The relevant process variables are the jet radius, axial velocity, charge distribution, and displacement of the centerline of the jet as a function of the axial distance from the nozzle. The full details of the theory will be presented elsewhere.¹⁵

Of crucial importance to understanding the electrospinning process is the competition between modes of instability. Whether whipping or axisymmetric breakup of the jet dominates for a given set of conditions depends on the jet radius and surface charge experienced by a fluid element as it travels downstream. Figure 3 plots the logarithm of the ratio of the maximum growth rates of the two conducting modes as a function of surface charge and jet radius for an aqueous solution of PEO. In the light region, the whipping mode is at least twice as unstable as the axisymmetric mode; in the dark

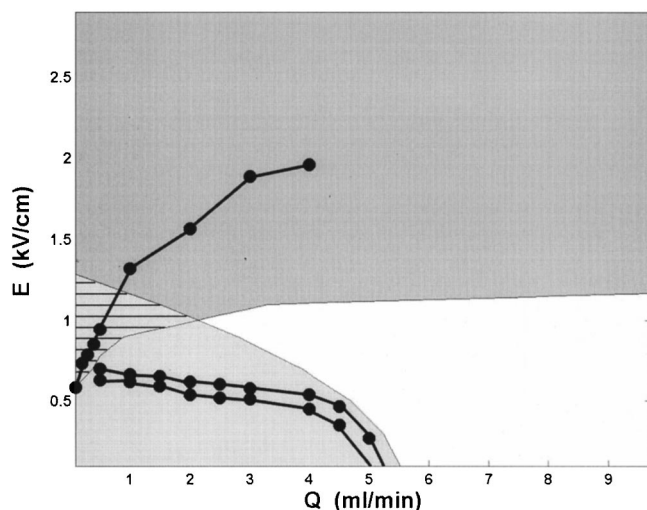


FIG. 4. Operating diagram showing stability transitions for a 2 wt % solution of PEO (MW=2 000 000) in water. Theoretical transitions are based on the contours of $\Gamma(E_\infty, Q) = 2\pi$. White region: theoretical steady jet; light gray region: theoretical Rayleigh unstable; dark gray region: theoretical whipping unstable; cross-hatched region: theoretical comparable instability to Rayleigh and whipping modes. Circles: experimental data.

region, this relative stability is inverted. In general, the whipping mode dominates at high charge density, whereas the axisymmetric mode dominates at low charge density. As a jet thins away from the nozzle, both the charge density and the radius change, thus tracing a path in this diagram.

The type of instability that is observed for a given set of experimental conditions can be computed by integrating the amplification factor for each mode of instability as it convects along the path of the jet from the nozzle to the collector. An asymptotic argument for a sufficiently thin jet, i.e., far from the nozzle, indicates that the path of the jet on the diagram in Fig. 3 ultimately approaches a straight line with unit slope and an intercept equal to $\ln(I/2Q)$, where I is the current and Q is the volumetric flow rate.^{15,16} Determining the jet path before it reaches this asymptotic regime requires solving the full electrohydrodynamic problem for the shape and charge distribution on the jet in the vicinity of the nozzle. By comparing theoretical solutions with experimental photographs of the jet shape, we found that quantitative agreement required a detailed analysis of the fringe fields in the vicinity of the nozzle. This procedure reveals the importance of nozzle design on the stability of the jet.

An “operating diagram” summarizes how the amplification factor $\Gamma(E_\infty, Q)$ for a particular instability depends on the applied electric field E_∞ and flow rate Q for a given set of fluid parameters. From the growth rate equation, we estimate $d \ln A/dt = \omega(h, E, \sigma)$, where $A(t)$ is the amplitude of a perturbation at time t . Approximating $dA/dt \sim U dA/dz$, where $U = Q/\pi h^2$, we obtain the amplification factor for a perturbation convected a distance d downstream:

$$\Gamma(E_\infty, Q) = \ln \left[\frac{A(d)}{A(0)} \right] = \int_0^d \frac{\omega(h, E, \sigma) \pi h^2}{Q} dz.$$

Only instabilities whose amplitudes have grown to a sufficient size will be observed. By plotting contour lines of the amplification factors for the various instability modes, we obtain a map of the jet behavior. Figure 4 shows a compar-

ison of theoretical and experimental operating diagrams for electrified jets of a PEO-water solution, spun over a distance of about 10 cm. A mild hysteresis is observed experimentally in the Rayleigh transition from unstable jets to stable jets at low field strength, which is not captured by the current theoretical analysis. At higher field strength and flow rate, we observe the transition from a stable jet to a whipping jet. The dependence of both transitions on the electric field and the flow rate is correctly reproduced by the model; this has also been confirmed for other fluids. Both the model and the experiments suggest that the whipping instability is responsible for the “inverse cone” envelope observed. The slight numerical discrepancies are no doubt due to the underlying approximations in our calculations. We conjecture that the whipping instability accounts for the large reduction in jet diameter by vastly increasing the path length over which the fluid is accelerated and stretched prior to solidification or impact on the collector. As an aside, we note that instabilities leading directly to multiple filaments, i.e., splaying, may also be considered within the current model framework by including higher moments in the multipole expansion for the charge distribution (quadrupoles, etc.) and developing asymptotic equations for the evolution of the jet shape.

The ideas presented here are both simple and appealing. The instability equations are relatively easy to solve, cover a wider range of materials and process parameters than previous studies, and are expressed in terms of well-known fluid properties. Our analysis focuses attention on the importance of jet shape and charge distribution in determining jet stability, and reveals the importance of equipment design, as manifested through the fringe fields at the nozzle, in determining the character of the instability.

The authors are grateful to L. P. Kadanoff, L. Mahadevan, D. Saville, D. Reneker, S. Warner, and I. Cohen for valuable discussions. Financial support was provided by the National Science Foundation (CTS-9457111, DMS-9733030, DMR-9808595, DMR-9728858), National Textile Center, Alfred P. Sloan Foundation, and the American Chemical Society (PR31941-G9).

- ¹R. Jaeger, M. M. Bergshoeff, C. Martin-i-Batlle, H. Schoenherr, and G. J. Vansco, *Macromol. Symp.* **127**, 141 (1998).
- ²P. Gibson, H. Schreuder-Gibson, and C. Pentheny, *J. Coated Fabr.* **28**, 63 (1998).
- ³J. S. Kim and D. H. Reneker, *Polym. Compos.* **20**, 124 (1999).
- ⁴L. Huang, R. A. McMillan, R. P. Apkarian, B. Pourdeyimi, V. P. Conicello, and E. L. Chaikof, *Macromolecules* **33**, 2899 (2000).
- ⁵P. K. Baumgarten, *J. Colloid Interface Sci.* **36**, 71 (1971).
- ⁶L. Larrondo and R. St. John Manley, *J. Polym. Sci., Part A-2* **19**, 909 (1981).
- ⁷J. Doshi and D. H. Reneker, *J. Electrostat.* **35**, 151 (1995).
- ⁸A. Ziabicki, *Fundamentals of Fibre Formation: The Science of Fiber Spinning and Drawing* (Wiley, New York, 1976).
- ⁹G. I. Taylor, *Proc. R. Soc. London, Ser. A* **280**, 383 (1964).
- ¹⁰S. B. Warner, A. Buer, S. C. Ugolue, G. C. Rutledge, and Y. M. Shin, *National Textile Center Annual Report No. 83-90* (1998).
- ¹¹D. H. Reneker, A. L. Yarin, H. Fong, and S. Koombhongse, *J. Appl. Phys.* **87**, 4531 (2000).
- ¹²G. I. Taylor, *Proc. R. Soc. London, Ser. A* **313**, 453 (1969).
- ¹³N. K. Nayyar and G. S. Murty, *Proc. Phys. Soc. London* **75**, 369 (1960).
- ¹⁴D. A. Saville, *Phys. Fluids* **13**, 2987 (1970).
- ¹⁵M. M. Hohman, Y. M. Shin, G. C. Rutledge, and M. P. Brenner, *Phys. Fluids* (to be published).
- ¹⁶V. N. Kirichenko, I. V. Petryanov-Sokolov, N. N. Suprun, and A. A. Shutov, *Sov. Phys. Dokl.* **31**, 611 (1986).